ACS APPLIED MATERIALS & INTERFACES

Research Article

www.acsami.org

Initiated Chemical Vapor Deposition (iCVD) of Highly Cross-Linked Polymer Films for Advanced Lithium-Ion Battery Separators

Youngmin Yoo,[†,∥] Byung Gon Kim,[‡,∥] Kwanyong Pak,[†] Sung Jae Han,[§] Heon-Sik Song,[§] Jang Wook Choi,[*,‡] and Sung Gap Im[*,†]

[†]Department of Chemical and Biomolecular Engineering and Graphene Research Center in KAIST Institute for NanoCentury and [‡]Graduate School of Energy, Environment, Water, and Sustainability (EEWS) and Center for Nature-inspired Technology (CNiT) in KAIST Institute for NanoCentury, Korea Advanced Institute of Science and Technology (KAIST), 291 Daehak-ro, Yuseong-gu, Daejeon 305-701, Republic of Korea

[§]IT&E R&D, LG Chem, Yuseong-gu, Daejeon 305-380, Republic of Korea

Supporting Information

ABSTRACT: We report an initiated chemical vapor deposition (iCVD) process to coat polyethylene (PE) separators in Li-ion batteries with a highly cross-linked, mechanically strong polymer, namely, polyhexavinyldisiloxane (pHVDS). The highly cross-linked but ultrathin pHVDS films can only be obtained by a vapor-phase process, because the pHVDS is insoluble in most solvents and thus infeasible with conventional solution-based methods. Moreover, even after the pHVDS coating, the initial porous structure of the separator is well preserved owing to the conformal vapor-phase deposition. The coating thickness is delicately controlled by deposition time to the level that the pore size decreases to below 7% compared to the original dimension. The pHVDS-coated PE shows substantially improved thermal stability and electrolyte wettability. After incubation at 140 °C for 30 min, the pHVDS-coated PE causes only a 12% areal shrinkage (versus 90% of the pristine separator). The superior wettability results in increased electrolyte uptake and ionic conductivity, leading to significantly improved rate performance. The current approach is applicable to a wide range of porous polymeric separators that suffer from thermal shrinkage and poor electrolyte wetting.

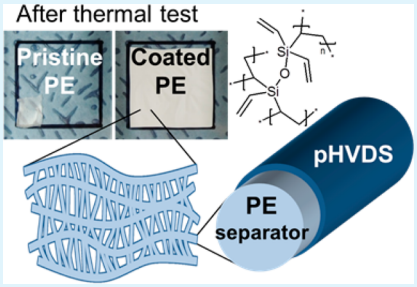

KEYWORDS: *initiated chemical vapor deposition (iCVD), Li-ion battery separator, poly hexavinyldisiloxane (pHVDS), thermal stability, electrolyte wettability*

1. INTRODUCTION

In the past several decades, a variety of rechargeable batteries have been developed to power diverse applications. Among them, lithium-ion batteries (LIBs) have lately received discernible attention due to their superior energy densities,[1−3] accelerating the advent of portable IT devices and electrified vehicles (EVs).[4−6] Nonetheless, the continuous increase of the energy density in LIBs has simultaneously raised the safety concern. Under overcharged states where oxygen can be evolved from cathode active materials, even microscale short circuits could trigger thermal runaway because of the flammable nature of commonly used electrolyte solvents. In the case of LIBs targeting large-scale applications such as EVs, this safety concern is more serious because each cell size is larger and a greater number of cells are required to be packed in a limited volume due to the demand on the high volumetric energy density.[3,7,8]

Separators can play a critical role in mitigating the safety problem as it can prevent short circuits between both electrodes and thus fatal thermal runaway. The most widely adopted separators are made of polyolefin-based polymers represented by polyethylene (PE) and polypropylene (PP). They have many advantages of low cost, good processability, and electrochemical stability.[9−12] However, they usually suffer from dimensional shrinkage at high temperatures due to the low melting points of those polymers (i.e., PE ≈ 135 °C)[11] and poor wetting with polar solvents used in current commercial electrolytes. The thermal shrinkage of separator is directly linked to the safety hazard because it could generate short circuits.

In an effort to overcome this shortcoming, many approaches have been introduced. Among them, the coating with ceramic particles on the separator surface is most representative.[13−15] The ceramic coating layers exert a resistance force against the dimensional shrinkage through their adhesion onto the separator. In spite of the success in minimizing the thermal shrinkage, the ceramic particle coating inevitably leads to an increase in the thickness, which is adverse to the current research effort to increase the volumetric energy density. As more sophisticated approaches in controlling the coating thickness, polydopamine (pD) coating[16] and alumina (Al_2O_3) coating employing atomic layer deposition (ALD) processes[17]

Received: June 26, 2015
Accepted: August 10, 2015
Published: August 10, 2015

DOI: 10.1021/acsami.5b05720
ACS Appl. Mater. Interfaces 2015, 7, 18849−18855

were also introduced. Although they represent a remarkable progress in the separator performance, the thickness control in the polydopamine coating is still hard to reach sub-10 nm resolution, and the extremely low throughput of the ALD process makes the process extremely challenging to be fully scalable. As alternative options to overcome the thermal shrinkage issue, a variety of nonwoven separators[18,19] were also developed. However, their pore sizes are usually too large to warrant short-circuit-free operations.

In the present study, in an attempt to improve the thermal stability of polyolefin separators and simultaneously enhance their inferior wettability with electrolytes, we introduce a new vapor-phase coating method, namely, an initiated chemical vapor deposition (iCVD) process,[20−22] to deposit a highly cross-linked polymer (polyhexavinyldisiloxane, pHVDS) conformally around the separator surface while keeping the increase of the separator thickness minimal. The pHVDS polymer can satisfy the requirements to improve cell performance such as thermal stability, mechanical robustness, good wettability with electrolytes, and electrochemical inertness. A main advantage of the iCVD process is the capability that an optimal coating thickness can be tuned precisely by controlling the deposition time in order to achieve improved thermal stability with minimal decrease of the pore size of the separator. Under such optimal coating, the resistance against thermal shrinkage and rate performance were markedly enhanced.

2. EXPERIMENTAL SECTION

2.1. Preparation of pHVDS-Coated PE Separator. The deposition of pHVDS on the PE separator (LG chem, Korea) was performed in an iCVD reactor (Daeki Hi-Tech Co., Ltd., Korea). The monomer, hexavinlydisiloxane (HVDS) (Gelest, USA), was heated to 40 °C, while the sufficiently volatile initiator, *tert*-butyl peroxide (TBPO) (Aldrich 98%, USA), was maintained at room temperature. The vaporized HVDS and TBPO were introduced into the iCVD reactor at flow rates of 1.2 and 0.6 sccm, respectively. Each flow rate was controlled by a needle valve. The chamber pressure of the iCVD reactor was maintained at 180 mTorr by a pressure controller (Genius, GT-400). The filament temperature was set to 200 °C, and the substrate temperature was held at 30 °C. The deposition time was varied from 20 (pHVDS-20 min PE) to 50 min (pHVDS-50 min PE). pHVDS was deposited on both sides of the separator. The shrinkage tests of the pristine and pHVDS-coated PE with a size of 2 cm × 2 cm were performed inside an oven at 140 °C for 30 min.

2.2. Preparation of pD- and Al_2O_3-Coated Separators. pD- and Al_2O_3-coated separators were also prepared to compare with the pDVDS-coated separator. For the pD coating, 50 mM dopamine hydrochloride (Aldrich, USA) was first dissolved in 80% methanol (Daejeong, Korea), and 1.5 equiv of $NaIO_4$ (Aldrich, USA) was added to the solution to oxidize dopamine. A 3 cm × 3 cm PE separator was then immersed in the dopamine solution during its polymerization for 1 day. Next, the pD-coated separator was washed with DI water and methanol three times and dried under vacuum at 70 °C for 24 h. The final pD loading density on the PE separator was on average 0.21 mg cm^{-2}. Al_2O_3-coated separator was fabricated using an ALD system (CN1 CO., Ltd., Korea). The chamber temperature was set to 90 °C. Trimethyl aluminum (TMA, UP chemical) was used for an Al precursor, and H_2O vapor (DI water) was used for a reactant. Each cycle of ALD consisted sequentially of injection of TMA for 0.3 s, 15 s of Ar purge, injection of H_2O vapor for 0.4 s, and another 15 s of Ar purge. The Al_2O_3 was deposited on both sides of the PE separator for 41 cycles. The final Al_2O_3 loading density on the PE separator was on average 0.13 mg cm^{-2}.

2.3. Characterization of pHVDS-Coated PE Separator. The elastic modulus of pHVDS polymer film was measured by a nanoindentation system (MTS Nano indenter XP, USA). The morphologies of the pristine and pHVDS-coated PE separators were monitored using field emission scanning electron microscopy (FE-SEM) (Hitachi S-4800, Japan). The elemental mapping of the pHVDS-coated PE separator was conducted using energy-dispersive X-ray spectroscopy (EDS) (Sirion, FEI, Netherlands). The chemical compositions and characters were analyzed by using X-ray photoelectron spectroscopy (XPS) (Sigma probe, Thermo VG Scientific, England) and Fourier transform infrared (FT-IR) (Alpha FT-IR Spectrometer, Bruker, USA) spectroscopy. The contact angle was measured with 5 μL of water droplets by using a contact angle analyzer (Phoenix 150, SEO, Korea). The electrolyte wettability was evaluated by dipping the tip of separator into the electrolyte (1 M $LiPF_6$ dissolved in ethylene carbonate (EC)/ethyl methyl carbonate (EMC) (1:2, v/v)). The thickness of separator was measured by using a height gauge (TESA-μhite, Switzerland). Average pore size and pores size distribution were measured by using a capillary flow porometer (PMI, CFP-1500AE, USA). For the analysis of the separators after electrochemical processes, the cells were disassembled and the separators were washed with ethanol and dried under vacuum for 24 h.

2.4. Electrochemical Tests. For preparation of the cathode, carbon-coated $LiFePO_4$ (LFP, average particle size = 500 nm) (Hanhwa Chemical Co., Ltd., Korea), Super P (TIMCAL, Switzerland), and poly(vinylidene fluoride) (PVDF) (Aldrich, Korea) were dispersed in *N*-methyl-2-pyrrolidone (NMP) (Aldrich, Korea) in a weight ratio of 8:1:1. Then the well-mixed slurry was cast onto Al foil using the doctor blade technique. The LFP loading density on the Al current collector was 1.4 mg cm^{-2}. For electrochemical characterization, the coin-type half-cells were used. In each cell, the LFP cathode, the pristine or modified separator, and Li foil (thickness = 600 μm, Honjo, Japan) were used as cathode, separator, and anode, respectively. All of the electrochemical tests were conducted using the electrolyte in which 1 M $LiPF_6$ is dissolved in cosolvents of EC and dimethyl carbonate (DMC) (1:1, v/v, Soulbrain Co., Ltd., Korea) in the voltage range of 2.4−4.2 V vs Li/Li^+. The unit cells were cycled at 0.1C (1C = 150 mA g^{-1}) and cycled at different C rates for rate performance test using a battery cycler (WonAtech, WBCS3000, Korea). In order to measure the ionic conductivity, electrochemical impedance spectroscopy (EIS) analysis (Biologic VSP battery cycler, France) was performed by using a sandwiched cell that locates the separator between two stainless steel plates in the frequency range from 10 mHz to 1 MHz. For the ionic conductivity measurement of the pHVDS polymer, the polymer was directly coated on one side of a stainless steel plate. The ionic conductivity (σ) of the sample could be calculated using, $\sigma = t/R_bA$, where t is the thickness of the sample, A is the area of the separator, and R_b is the bulk resistance. All of the electrochemical tests were conducted at room temperature.

3. RESULTS AND DISCUSSION

3.1. pHVDS Coating on PE Separator via iCVD Process. During the iCVD process, TBPO is thermally decomposed to radicals and subsequently initiates radical polymerization of HVDS to form highly cross-linked polymer, pHVDS[23] on a PE separator, placed on a cooled substrate in the iCVD system (Figure 1). The deposited pHVDS film maintains its mechanical stability and flexibility based on both the densely cross-linked polymer network and the flexible, linear Si−O linkage.[23] Due to this highly cross-linked structure, the elastic modulus of pHVDS film was measured to be 6.31 GPa, which is an order of magnitude larger than that (0.635 GPa) of the pristine PE. Also, the pHVDS film is not liable to dissolution to commonly used solvents such as isopropyl alcohol (IPA) and acetone. This chemical stability, in turn, indicates that the formation of a thin pHVDS film is not feasible by conventional solution-based processes. By contrast, the vapor-phase deposition method allows one to produce a conformal pHVDS film via an in situ polymerization of HVDS monomer because the initiation and subsequent polymerization all take place in the vapor phase. Furthermore, the film

DOI: 10.1021/acsami.5b05720
ACS Appl. Mater. Interfaces 2015, 7, 18849−18855

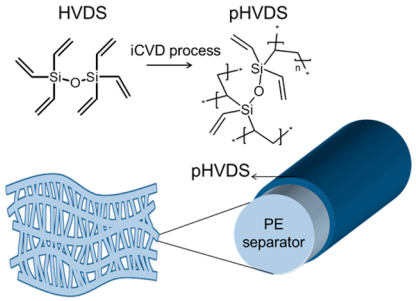

Figure 1. Schematic image of pHVDS-coated PE separator. HVDS monomer was polymerized by an iCVD process to conformally deposit cross-linked polymer, pHVDS, on the PE separator.

thickness can be tuned by controlling the deposition time. For example, the deposition time in our experiment was controlled to be 40 min to limit the pore size decrease below 7% with respect to that of the pristine separator (Figure S1a). The coating thickness was estimated by obtaining the pore size difference before and after the pHVDS coating. According to capillary flow porometer measurement (Figure S1b), the pore size of pHVDS-40 min PE was measured as 77.8 ± 1.9 nm while the pristine PE was measured as 85.6 ± 1.5 nm. In this porometer analysis, it should be noted that the pore size is underestimated compared to the actual value because the analysis reads the pore size at the most constricted part, so-called the throat diameter, along the pore channel. For the same reason, the coating thicknesses are also underestimated. In addition, the capillary flow porometer measurement informs rough pore size of each separator near the average value but does not provide detailed information on pore shape, as random pore shapes are illustrated by SEM analysis in Figure 2. The difference of pore size between pristine PE and pHVDS-40 min PE was approximately 7.8 nm. Since the pHVDS covers the whole surface of each pore, the coating thickness can be

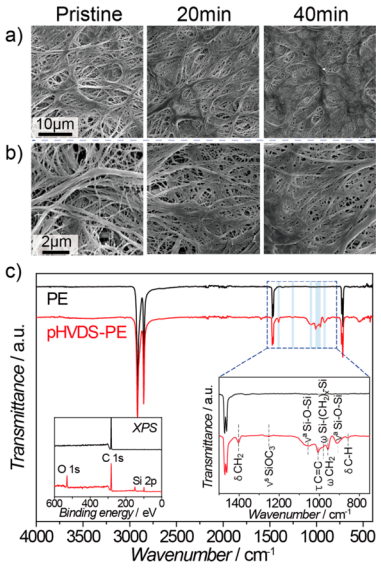

Figure 2. SEM images of PE separators in (a) low and (b) high magnifications after different deposition times. (c) FT-IR and XPS spectra (left inset) of the pristine PE separator (black) and pHVDS-coated PE separator (red). Right inset image is an enlarged view of FT-IR spectra in the region of 750−1500 cm^{-1} (ν, stretching; δ, bending; ω, wagging; τ, twisting; a, asymmetric; s, symmetric).

calculated to be one-half of the pore size difference, which is ~3.9 nm, assuring the thickness control of the iCVD process without blocking the pores.

In order to investigate the surface morphology and the chemical composition of pHVDS, SEM, FT-IR, and XPS analyses were performed. As displayed in Figure 2a and 2b, the SEM images of the pristine and pHVDS-coated PE separators at various coating times show that although the pore size becomes slightly smaller with the deposition time the original porous structure of the PE separator remains to a large extent.

The chemical bonding characteristics of the pHVDS coating layer were monitored by FT-IR analyses (Figure 2c). The FT-IR spectrum of the pristine PE separator shows only characteristic peaks of PE at 2918, 2848, 1468, and 718 cm^{-1},[24] corresponding to asymmetric, symmetric stretching of C−H bond in CH_2 groups, scissoring, and rocking of CH_2, respectively. By contrast, the spectrum of the pHVDS-coated PE separator exhibits new peaks, reflective of pHVDS formation. The blue shades in the FT-IR spectra cover the peaks at 1404, 1254, 1055, and 989 cm^{-1} assigned to the bending of CH_2 in Si−$(CH_2)_x$−Si, symmetric stretch of $SiOC_3$, asymmetric stretch of Si−O−Si, and wagging of Si−$(CH_2)_x$−Si, respectively.[25] Also, the deposition of pHVDS layer of PE separator is also confirmed by the XPS spectra. While the XPS spectrum of pristine PE separator shows only a C 1s peak, that of the pHVDS-coated one exhibits O 1s and Si 2p peaks at 532 and 101 eV, respectively, in addition to the C 1s peak at 284.5 eV. The basic physical properties of the pristine PE, pHVDS-20 min PE, and pHVDS-40 min PE are summarized in Table S1 in the Supporting Information.

3.2. Thermal Stability of pHVDS-Coated PE Separator.

In order to assess the thermal stability of the pHVDS-coated PE separator, the pristine and pHVDS-coated PE with a size of 2 cm × 2 cm were located in an oven at 140 °C for 30 min. The dimensional change of each separator was quantified, as shown in Figure 3a. The pristine PE and pHVDS-20 min PE became slightly transparent by the thermal treatment, most likely due to the blocked pores by thermal deformation of the pristine PE separator, which would decrease the light scattering effect by the pores in the separator (Figure 3b). In contrast, pHVDS-40 min PE did not show any apparent morphological change even after the same thermal treatment owing to the well-preserved porous structure. As summarized in Figure 3c, pHVDS-40 min PE retained 87.8% of its initial area, while the pristine one and pHVDS-20 min PE underwent substantial thermal shrinkage to leave only 10.0% and 28.5% of its initial area, respectively. On the other hand, the excessive deposition decays electrochemical performance. For example, although the thermal shrinkage of the pHVDS-50 min PE dropped to 6.2% (Figure S3), its electrolyte uptake was impaired significantly because of the decreased pore size. On the basis of this observation, pHVDS-40 min PE was selected as a main sample for comprehensive electrochemical testing in the present study (Figure S4). This observation implies a trade-off relation between thermal stability and ionic conductivity that is critically associated with other electrochemical properties. The differential scanning calorimetry (DSC) result was also consistent with the thermal shrinkage result, as the pHVDS-coated separators with longer deposition times showed higher melting points due to the thermally stable pHVDS polymer coating as compared to that of the pristine counterpart (Figure S5). In order to confirm the thermal stability of the pHVDS-coated separators, several coating methods, such as Al_2O_3 coating via ALD process and

DOI: 10.1021/acsami.5b05720
ACS Appl. Mater. Interfaces 2015, 7, 18849−18855

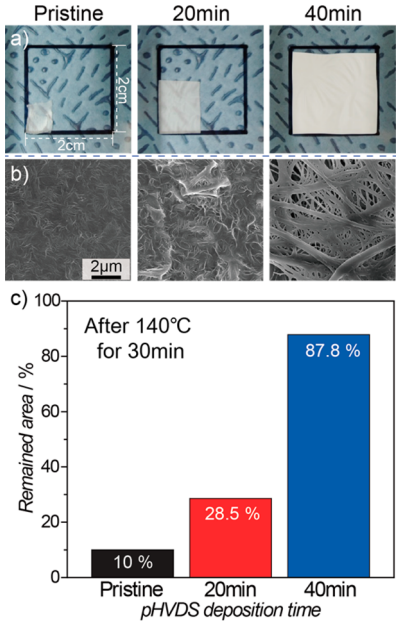

Figure 3. (a) Thermal shrinkage and (b) SEM images of the pristine PE (left), pHVDS-20 min PE (middle), and pHVDS-40 min PE (right) after storage at 140 °C for 30 min. (c) Areal shrinkage of each separator.

pD coating, were compared (Figure S6). After the same thermal treatment at 140 °C for 30 min, the pHVDS-50 min PE maintained its original dimensions, whereas the areas of the Al_2O_3-coated PE and pD-coated PE shrank by 56.0% and 30.5%, respectively, reconfirming the superior thermal stability of the pHVDS coating.

3.3. Wettability of pHVDS-Coated PE Separator. The wettability of the separator was also examined before and after the pHVDS coating (Figure 4a and 4b). The water contact

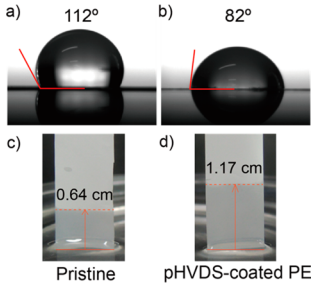

Figure 4. Water contact angles of (a) the pristine PE and (b) pHVDS-40 min PE. Electrolyte wettability tests of (c) the pristine separator and (d) pHVDS-40 min PE. Tips of both separators were contacted with the electrolyte at t = 0. Pictures were taken at t = 2 h.

angles of the pristine one and pHVDS-40 min were 112° and 82°, respectively, indicating the enhanced hydrophilic nature of the pHVDS-coated surface. While PE is composed of only methyl group which generally shows hydrophobic property, pHVDS contains disiloxane and methyl and vinyl groups, which makes the pHVDS polymer more hydrophilic. The wettability with an LIB electrolyte (1 M $LiPF_6$ in EC: EMC (1:2, v/v)) was also tested (Figure 4c and 4d). When the tip of the separator was dipped in the electrolyte for 2 h, the electrolyte absorption proceeded over 1.17 cm for pHVDS-40 min, which is in contrast with that (0.64 cm) of the pristine separator. These distinct results between both samples indicate that the electrolyte uptake is determined by the surface properties of the separator, and the pHVDS coating improves the wettability markedly. The enhanced wettability was also reflected in the higher ionic conductivities of the pHVDS-coated separators (Figure S7).[26,27] Although the measured ionic conductivity of the nonporous pHVDS polymer itself is quite low (8.7×10^{-6} S cm^{-1}) (Figure S8), the value of the coated separator increased from 6.6×10^{-4} to 8.4×10^{-4} S cm^{-1} by facilitated ionic transport via the enhanced electrolyte wetting in the presence of porosity. The enhanced separator−electrolyte interaction is attributed to the relatively polar Si−O−Si group in the HVDS.

3.4. Electrochemical Performance of pHVDS-Coated PE Separator. In order to evaluate the pHVDS coating effect on the electrochemical performance, coin-type half-cells were prepared. To focus explicitly on separator effects, carbon-coated LFP was chosen as an active material because its structural stability during cycling has been warranted.[28−30] In addition, for fair comparison, the electrolyte amount was controlled to be identical at 0.3 mL in all coin cells.[31]

The first voltage profiles of the cells using various separators are displayed in Figure 5a. These profiles were obtained based on the scanning condition at 0.1C (1C = 150 mA g^{-1}) in the

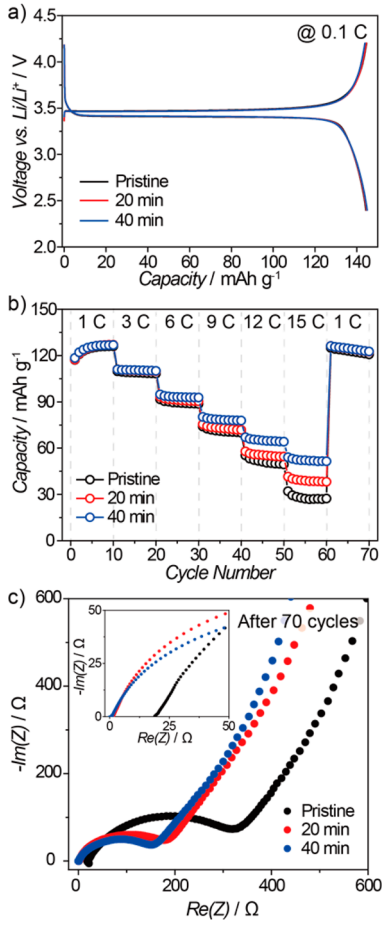

Figure 5. Electrochemical characterization for the cells with and without the pHVDS coating on PE separators. (a) Voltage profiles of the cells with the pristine and pHVDS-coated PE during the first cycle at 0.1C (1C = 150 mA g^{-1}) in the voltage range of 2.4−4.2 V. (b) Rate performance tests for all cells at different C rates from 1C to 15C. (c) Nyquist plots for all cells measured after the 70 cycles shown in b. (Inset) The same Nyquist plots magnified near the origin.

DOI: 10.1021/acsami.5b05720
ACS Appl. Mater. Interfaces 2015, 7, 18849−18855

voltage range of 2.4−4.2 V. Clear flat voltage plateaus around 3.4 V, which is characteristic of LFP, were observed both charging and discharging processes.[28,29] The capacities and Coulombic efficiencies in the first cycles were almost identical for all three cells, suggesting that the pHVDS coating is electrochemically stable in the given potential window.[32,33]

In order to monitor the pHVDS coating effect on the rate performance, the cells were cycle tested at different C rates from 1C to 15C (1C = 150 mA g^{-1}) (Figure 5b and S9). While the discharging capacity of the cell with the pristine separator dropped from 126 to 27.2 mAh g^{-1} upon the C-rate increase from 1C to 15C, the cell with pHVDS-40 min PE exhibited almost a two times higher capacity of 51.4 mAh g^{-1}, corresponding to a 40.5% retention as compared to the value at 1C (126.8 mAh g^{-1}). The superior rate performance of pHVDS-40 min is attributed to the higher ionic conductivity of the pHVDS-coated separator.

To further investigate the role of pHVDS-40 min PE to the enhanced rate capability of the cell, EIS tests were carried out to the cell before and after the 70 cycles dedicated for the rate performance tests, which is shown in Figure 5b (Figure S10 for the Nyquist plots before cycling). The spectra consist of a semicircle in the high−middle-frequency regions and a straight line in the low-frequency region (Figure 5c). According to other similar investigations,[16,27,34−38] the semicircle in the high−middle-frequency region is associated with combined phenomena of Li-ion diffusion in the solid electrolyte interphase (SEI) layer (R_{SEI}) and charge transfer process (R_{ct}). The *x*-axis intercept corresponds to the bulk resistance (R_b) from the electrolyte and electrode.[27,34] After the 70 cycles, the pHVDS-coated PE cell showed lower R_b than that of the pristine PE cell due to the enhanced ionic conductivity by the increased electrolyte uptake and retention of the separator.[27,34,35] The pHVDS-coated PE cell exhibited lower interfacial resistance ($R_i = R_{SEI} + R_{ct}$) than that of the pristine PE cell, which can be interpreted in a way that the enhanced electrolyte uptake and retention also facilitate Li-ion diffusion at the electrode−electrolyte interface.[16,24,32−34] The superior rate capability of pHVDS-coated PE is ascribed to the reduction in these resistances leading to the lower overpotentials (Figure S9). However, pHVDS-50 min PE showed lower ionic conductivity (Figure S7) and higher R_i (Figure S11) than those of the pHVDS-40 min PE, presumably due to the decreased porosity, which may also be the reason for the inferior rate capability (Figure S11). The high thermal stability of the pHVDS-coated PE was also reflected in the impedance spectra (Figure S12) showing significantly lower total resistance after heat treatment (140 °C, 30 min) compared to that of the pristine. The blocked pore of the pristine PE after heat treatment is the main origin for the higher resistance of the pristine PE.

3.5. Stability of pHVDS-Coated PE Separator after Electrochemical Tests. The stability of the pHVDS-coated separators was also assessed after the cycling test. To this end, the separators coated with pHVDS for various durations were analyzed by using SEM, FT-IR, and XPS after the rate performance tests for 70 cycles. According to the SEM images (Figure 6a and 6b), the morphologies of the pore structures were well preserved for all three cases compared with those before cycling (Figure 2a). No delamination or cracks of the pHVDS layer on PE separator was observed after the 70-cycle test (Figure S13). The FT-IR spectra also did not show any apparent difference from that before the same cycling process.

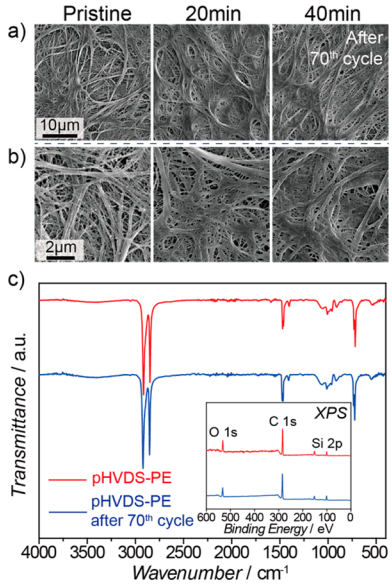

Figure 6. (a and b) SEM images of the pristine PE (left), pHVDS-20 min PE (middle), and pHVDS-40 min PE (right) after the 70 cycles shown in Figure 5b at (a) low (×5000) and (b) high (×20 000) magnification. (c) FT-IR and XPS spectra (inset) of pHVDS-40 min PE before and after the same 70 cycles.

It was also confirmed that after 70 cycles, the original Si 2p and O 1s peaks were well maintained in XPS results (inset, Figure 6c). These series of data demonstrate the robust character of the pHVDS coating layer and its sustainable effect on the electrochemical properties during repeated charge−discharge cycles.

CONCLUSION

In summary, we introduced a thin, conformal pHVDS polymer coating on PE separators using an iCVD process. The vapor-phase reaction in the iCVD process allows one to deposit pHVDS that would be highly challenging to be processed into a thin film under any conventional solution-based methods, with exquisite thickness controllability by tuning its deposition time. The pHVDS coating resolves the chronic thermal shrinkage problem of the current commercial PE separators by the polymeric network and intrinsic mechanical stability of pHVDS, validating the coating effect toward safer cell operations. The polarity of pHVDS also enhances the wettability with LIB electrolytes, leading to improved rate performance as compared with that of the pristine separator without such treatment. The current approach is independent of substrate materials and should thus be versatile to other LIB separators. Furthermore, other iCVD polymers beyond pHVDS should also be applicable to post-LIBs where the role of separators becomes very critical.

ASSOCIATED CONTENT

Supporting Information

The Supporting Information is available free of charge on the ACS Publications website at DOI: 10.1021/acsami.5b05720.

More pores size information, basic properties of separators, EDAX images, digital camera and SEM images after heat treatments, DSC data, additional results regarding thermal shrinkage, electrolyte uptake, ionic conductivity, electrochemical performance (PDF)

DOI: 10.1021/acsami.5b05720
ACS Appl. Mater. Interfaces 2015, 7, 18849−18855

AUTHOR INFORMATION

Corresponding Authors

*E-mail: jangwookchoi@kaist.ac.kr. Fax: +82-42-350-2248.
*E-mail: sgim@kaist.ac.kr. Fax: +82-42-350-3910.

Author Contributions

[‖]These authors contributed equally. The manuscript was written through contributions of all authors. All authors have given approval to the final version of the manuscript.

Notes

The authors declare no competing financial interest.

ACKNOWLEDGMENTS

This work was supported by the LG chem. J.W.C. acknowledges financial support by the National Research Foundation of Korea (NRF) Grant funded by the Korea government (MEST, NRF-2012-R1A2A1A01011970). B.G.K. acknowledges the NRF-2013-Global Ph.D Fellowship Program.

REFERENCES

(1) Tarascon, J. M.; Armand, M. Issues and Challenges Facing Rechargeable Lithium Batteries. *Nature* **2001**, *414* (6861), 359−367.
(2) Li, H.; Wang, Z. X.; Chen, L. Q.; Huang, X. J. Research on Advanced Materials for Li-ion Batteries. *Adv. Mater.* **2009**, *21* (45), 4593−4607.
(3) Hassoun, J.; Panero, S.; Reale, P.; Scrosati, B. A New, Safe, High-Rate and High-Energy Polymer Lithium-Ion Battery. *Adv. Mater.* **2009**, *21* (47), 4807−4810.
(4) Lu, L. G.; Han, X. B.; Li, J. Q.; Hua, J. F.; Ouyang, M. G. A Review on the Key Issues for Lithium-ion Battery Management in Electric Vehicles. *J. Power Sources* **2013**, *226*, 272−288.
(5) Kang, B.; Ceder, G. Battery Materials for Ultrafast Charging and Discharging. *Nature* **2009**, *458* (7235), 190−193.
(6) Armand, M.; Tarascon, J. M. Building Better Batteries. *Nature* **2008**, *451* (7179), 652−657.
(7) Goodenough, J. B.; Kim, Y. Challenges for Rechargeable Li Batteries. *Chem. Mater.* **2010**, *22* (3), 587−603.
(8) Liu, C.; Li, F.; Ma, L. P.; Cheng, H. M. Advanced Materials for Energy Storage. *Adv. Mater.* **2010**, *22* (8), E28−E62.
(9) Zhang, S. S. A Review on the Separators of Liquid Electrolyte Li-ion Batteries. *J. Power Sources* **2007**, *164* (1), 351−364.
(10) Venugopal, G.; Moore, J.; Howard, J.; Pendalwar, S. Characterization of Microporous Separators for Lithium-ion Batteries. *J. Power Sources* **1999**, *77* (1), 34−41.
(11) Zhang, J. J.; Liu, Z. H.; Kong, Q. S.; Zhang, C. J.; Pang, S. P.; Yue, L. P.; Wang, X. J.; Yao, J. H.; Cui, G. L. Renewable and Superior Thermal-Resistant Cellulose-Based Composite Nonwoven as Lithium-Ion Battery Separator. *ACS Appl. Mater. Interfaces* **2013**, *5* (1), 128−134.
(12) Arora, P.; Zhang, Z. M. Battery Separators. *Chem. Rev.* **2004**, *104* (10), 4419−4462.
(13) Jeong, H. S.; Lee, S. Y. Closely Packed SiO_2 Nanoparticles/Poly(vinylidene fluoride-hexafluoropropylene) Layers-coated Polyethylene Separators for Lithium-ion Batteries. *J. Power Sources* **2011**, *196* (16), 6716−6722.
(14) Cho, T. H.; Tanaka, M.; Ohnishi, H.; Kondo, Y.; Yoshikazu, M.; Nakamura, T.; Sakai, T. Composite Nonwoven Separator for Lithium-ion Battery: Development and Characterization. *J. Power Sources* **2010**, *195* (13), 4272−4277.
(15) Shin, W. K.; Kim, D. W. High Performance Ceramic-coated Separators Prepared with Lithium Ion-containing SiO_2 Particles for Lithium-ion Batteries. *J. Power Sources* **2013**, *226*, 54−60.
(16) Ryou, M. H.; Lee, D. J.; Lee, J. N.; Lee, Y. M.; Park, J. K.; Choi, J. W. Excellent Cycle Life of Lithium-Metal Anodes in Lithium-Ion Batteries with Mussel-Inspired Polydopamine-Coated Separators. *Adv. Energy Mater.* **2012**, *2* (6), 645−650.
(17) Jung, Y. S.; Cavanagh, A. S.; Gedvilas, L.; Widjonarko, N. E.; Scott, I. D.; Lee, S. H.; Kim, G. H.; George, S. M.; Dillon, A. C. Improved Functionality of Lithium-Ion Batteries Enabled by Atomic Layer Deposition on the Porous Microstructure of Polymer Separators and Coating Electrodes. *Adv. Energy Mater.* **2012**, *2* (8), 1022−1027.
(18) Choi, E. S.; Lee, S. Y. Particle Size-dependent, Tunable Porous Structure of a SiO_2/poly(vinylidene fluoride-hexafluoropropylene)-coated Poly(ethylene terephthalate) Nonwoven Composite Separator for a Lithium-ion Battery. *J. Mater. Chem.* **2011**, *21* (38), 14747−14754.
(19) Orendorff, C. J.; Lambert, T. N.; Chavez, C. A.; Bencomo, M.; Fenton, K. R. Polyester Separators for Lithium-Ion Cells: Improving Thermal Stability and Abuse Tolerance. *Adv. Energy Mater.* **2013**, *3* (3), 314−320.
(20) Im, S. G.; Gleason, K. K. Solvent-free Modification of Surfaces with Polymers: The Case for Initiated and Oxidative Chemical Vapor Deposition (CVD). *AIChE J.* **2011**, *57* (2), 276−285.
(21) Yoo, Y.; You, J. B.; Choi, W.; Im, S. G.; Stacked, A. Polymer Film for Robust Superhydrophobic Fabrics. *Polym. Chem.* **2013**, *4* (5), 1664−1671.
(22) Yoo, G.; Yoo, Y.; Kwon, J. H.; Darpito, C.; Mishra, S. K.; Pak, K.; Park, M. S.; Im, S. G.; Yang, J. W. An Effective, Cost-efficient Extraction Method of Biomass from Wet Microalgae with a Functional Polymeric Membrane. *Green Chem.* **2014**, *16* (1), 312−319.
(23) Coclite, A. M.; Ozaydin-Ince, G.; d'Agostino, R.; Gleason, K. K. Flexible Cross-Linked Organosilicon Thin Films by Initiated Chemical Vapor Deposition. *Macromolecules* **2009**, *42* (21), 8138−8145.
(24) Kim, B. G.; Kim, S.; Lee, H.; Choi, J. W. Wisdom from the Human Eye: A Synthetic Melanin Radical Scavenger for Improved Cycle Life of Li-O_2 Battery. *Chem. Mater.* **2014**, *26* (16), 4757−4764.
(25) Rau, C.; Kulisch, W. Mechanisms of Plasma Polymerization of Various Silico-Organic Monomers. *Thin Solid Films* **1994**, *249* (1), 28−37.
(26) Kim, D. W.; Ko, J. M.; Chun, J. H.; Kim, S. H.; Park, J. K. Electrochemical Performances of Lithium-ion Cells Prepared with Polyethylene Oxide-coated Separators. *Electrochem. Commun.* **2001**, *3* (10), 535−538.
(27) Ryou, M. H.; Lee, Y. M.; Park, J. K.; Choi, J. W. Mussel-Inspired Polydopamine-Treated Polyethylene Separators for High-Power Li-Ion Batteries. *Adv. Mater.* **2011**, *23* (27), 3066−3070.
(28) Yamada, A.; Chung, S. C.; Hinokuma, K. Optimized $LiFePO_4$ for Lithium Battery Cathodes. *J. Electrochem. Soc.* **2001**, *148* (3), A224−A229.
(29) Padhi, A. K.; Nanjundaswamy, K. S.; Goodenough, J. B. Phospho-olivines as Positive-electrode Materials for Rechargeable Lithium Batteries. *J. Electrochem. Soc.* **1997**, *144* (4), 1188−1194.
(30) Wang, J. J.; Sun, X. L. Olivine $LiFePO_4$: the Remaining Challenges for Future Energy Storage. *Energy Environ. Sci.* **2015**, *8* (4), 1110−1138.
(31) Ko, J. M.; Min, B. G.; Kim, D. W.; Ryu, K. S.; Kim, K. M.; Lee, Y. G.; Chang, S. H. Thin-film Type Li-ion Battery, Using a Polyethylene Separator Grafted with Glycidyl Methacrylate. *Electrochim. Acta* **2004**, *50* (2−3), 367−370.
(32) Dey, A. N.; Sullivan, B. P. Electrochemical Decomposition of Propylene Carbonate on Graphite. *J. Electrochem. Soc.* **1970**, *117* (2), 222−224.
(33) He, Y.; Yu, X. Q.; Wang, Y. H.; Li, H.; Huang, X. J. Alumina-Coated Patterned Amorphous Silicon as the Anode for a Lithium-Ion Battery with High Coulombic Efficiency. *Adv. Mater.* **2011**, *23* (42), 4938−4941.
(34) Cho, T. H.; Tanaka, M.; Onishi, H.; Kondo, Y.; Nakamura, T.; Yamazaki, H.; Tanase, S.; Sakai, T. Battery Performances and Thermal Stability of Polyacrylonitrile Nano-fiber-based Nonwoven Separators for Li-ion Battery. *J. Power Sources* **2008**, *181* (1), 155−160.
(35) Lee, T.; Lee, Y.; Ryou, M. H.; Lee, Y. M. A Facile Approach to Prepare Biomimetic Composite Separators Toward Safety-enhanced Lithium Secondary Batteries. *RSC Adv.* **2015**, *5* (49), 39392−39398.
(36) Chen, Z. H.; Zhang, L. Z.; West, R.; Amine, K. Gel Electrolyte for Lithium-ion Batteries. *Electrochim. Acta* **2008**, *53* (8), 3262−3266.

DOI: 10.1021/acsami.5b05720
ACS Appl. Mater. Interfaces 2015, 7, 18849−18855

(37) Jeong, Y. B.; Kim, D. W. Effect of Thickness of Coating Layer on Polymer-coated Separator on Cycling Performance of Lithium-ion Polymer Cells. *J. Power Sources* **2004**, *128* (2), 256−262.
(38) Kim, B. G.; Lee, J. N.; Lee, D. J.; Park, J. K.; Choi, J. W. Robust Cycling of LiO_2 Batteries through the Synergistic Effect of Blended Electrolytes. *ChemSusChem* **2013**, *6* (3), 443−448.

DOI: 10.1021/acsami.5b05720
ACS Appl. Mater. Interfaces 2015, 7, 18849−18855